Pergamon

Geochimica et Cosmochimica Acta, Vol. 68, No. 1, pp. 47–59, 2004

0016-7037/04 $30.00 + .00

doi:10.1016/S0016-7037(03)00260-6

Calcium carbonate dissolution in deep sea sediments: Reconciling microelectrode, pore water and benthic flux chamber results

RICHARD A. JAHNKE* and DEBORAH B. JAHNKE
Skidaway Institute of Oceanography, 10 Ocean Science Circle, Savannah, GA 31411

(*Received October* 14, 2002; revised 8 April 2003; *accepted in revised form April* 8, 2003)

Abstract—We report the benthic fluxes of O_2, titration alkalinity (TA), Ca^{2+}, NO_3^-, PO_4^{3-}, and $Si(OH)_4$ from in situ benthic flux chamber incubations on the Ceara Rise and Cape Verde Plateau and compare them to previously published results. We find within analytical uncertainty that the TA flux is twice the calcium flux, suggesting that dissolution/precipitation of $CaCO_3$ is the principal mechanism controlling benthic TA and Ca^{2+} fluxes. At sites where the sediments contain significant (>35%) $CaCO_3$ and the overlying waters are supersaturated with respect to $CaCO_3$, the ratios of the total dissolution rate to the remineralization rate are significantly less than at all other study sites. We propose that these observations can be explained by precipitation of fresh $CaCO_3$ at the supersaturated sediment surface followed by redissolution deeper in the sediments because of metabolically-produced CO_2. A numerical simulation is presented to demonstrate the feasibility of this explanation. In addition, surface exchange reactions in high-$CaCO_3$ sediments coupled with high rates of particle mixing may also impact rates of metabolic dissolution and depress chamber-derived estimates of carbonate alkalinity and calcium benthic fluxes. These results suggest that at supersaturated, high $CaCO_3$ locations, previous models of sediment diagenesis may have overestimated the impact of metabolic dissolution on the preservation of $CaCO_3$ deposited on the sea floor.

1. INTRODUCTION

The development of a fundamental and accurate understanding of the processes controlling the dissolution of $CaCO_3$ at the sea floor remains an important goal for marine geochemistry. It has been proposed that sea floor $CaCO_3$ dissolution may influence atmospheric CO_2 concentrations on glacial to interglacial time scales (Archer and Maier-Reimer, 1994) and will neutralize the anthropogenic CO_2 currently accumulating through surface ocean gas exchange or potentially directly injected into the deep ocean in the future. Furthermore, an accurate interpretation of the marine sediment record requires that the processes controlling the preservation of $CaCO_3$ be known (Milliman et al., 1999).

$CaCO_3$ dissolution rates in sediments are controlled by the solubility and kinetic characteristics intrinsic to the mineral and by external processes that control the saturation state of the surrounding fluids. Biogenically-produced $CaCO_3$ particles typically have very large surface areas due to the presence of pores in foraminiferal tests and coccolithophorid plates which may be increasingly exposed to pore waters as the primary particles are broken and dissolution proceeds. Although questions remain concerning the solubility and kinetic characteristics of $CaCO_3$ minerals in seawater (e.g., Hales, 1995; Hales and Emerson, 1996, 1997b), we focus here on the diagenetic and transport processes controlling the saturation state of pore waters and their impact on overall sea floor dissolution.

Previous studies of net sea floor $CaCO_3$ dissolution have assumed that dissolution is driven by undersaturation in the pore waters due to solute exchange with undersaturated bottom waters (inorganic dissolution) and by metabolic processes within the sediments (such as CO_2 production due to respiration or the re-oxidation of reduced metabolites such as Fe^{2+}, Mn^{2+}, or S^{2-}; metabolic dissolution; Emerson and Bender, 1981). Reduced secondary metabolites are generally of minor importance at most of the open ocean sites discussed in this manuscript. For simplification, therefore, we will describe metabolic dissolution solely in terms of metabolic CO_2 recognizing that these other reactants may also contribute.

Above the saturation horizon, it appears that essentially all sedimentary dissolution is attributed to metabolic dissolution. Dissolution of $CaCO_3$ particles within organism guts may occur independent of the saturation state of the surrounding waters (Milliman et al., 1999). While this may be an important process within the water column, at the deep sea floor we presently have little evidence that this process contributes significantly to the total dissolution rate. Also, less stable $CaCO_3$ phases (e.g., biogenic, high-Mg calcites) may dissolve above the calcite saturation horizon but unless significant amounts are exported from shallow environments, they are not likely to dominate deep-sea fluxes. Although supersaturated conditions at the sediment surface exist, direct inorganic precipitation of $CaCO_3$ has not been considered even though it has been documented to occur in supersaturated surface waters (Broecker and Takahashi, 1966; Morse et al., in press).

When bottom waters are undersaturated, the relative roles of inorganic and metabolic dissolution are controlled by relative rates of metabolic CO_2 production, pore water–overlying water solute exchange and $CaCO_3$ mineral dissolution kinetics. Metabolic dissolution is favored when solute exchange rates are slow and/or mineral dissolution kinetics are rapid. Under these conditions metabolically produced CO_2 will have a high probability of reacting with the solid phase $CaCO_3$ and metabolic dissolution is defined to be highly efficient—that is, the majority of the CO_2 produced is neutralized through $CaCO_3$ dissolution. On the other hand, if dissolution rates are slow and/or

* Author to whom correspondence should be addressed (rick@skio.peachnet.edu).

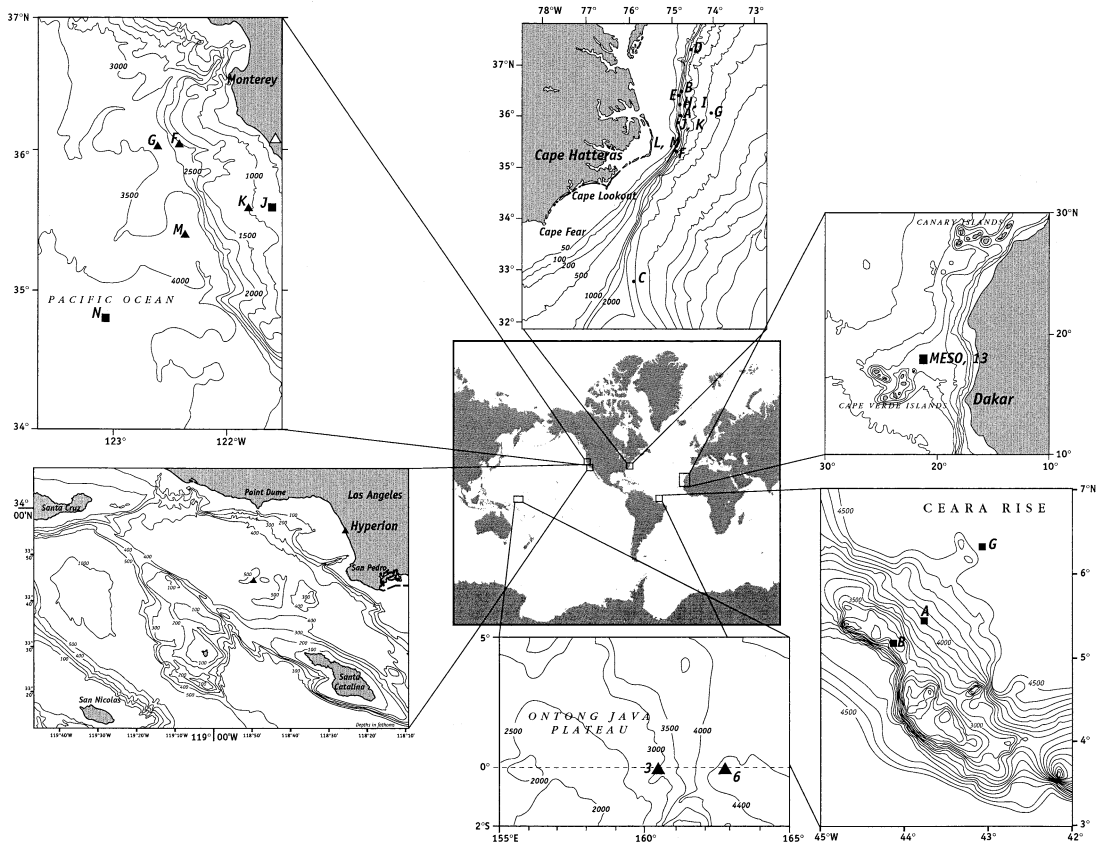

Fig. 1. In situ benthic flux chamber deployment locations.

solute exchange with the overlying water is rapid, metabolically produced CO_2 will have a higher probability of being transported out of the pore waters or being neutralized by CO_3^{2-} ions transported into the pore waters from the bottom waters before reacting with the solid phase and metabolic dissolution is reduced. Here, the efficiency of metabolic dissolution is defined to be low, with the majority of the CO_2 produced not reacting with the solids.

Evidence for the occurrence of metabolic dissolution has been provided by numerous studies of pore water chemical and carbon isotopic gradients (Archer, 1991; Hales and Emerson, 1996, 1997a; Martin and Sayles, 1996; Gehlen et al., 1999; and others) and through in situ benthic flux chamber incubations (Jahnke et al., 1997; Jahnke and Jahnke, 2000). The early calculations and many of the pore water results suggest that metabolic dissolution is highly efficient, with the majority of the metabolically-produced CO_2 driving dissolution (Emerson and Bender, 1981; Archer, 1991; Martin and Sayles, 1996). High metabolic efficiency implies that the rain rate of organic matter to the sea floor exerts a major control on sea floor dissolution, that significant dissolution within the sediments occurs above the saturation horizon and that only modest differences (factor of 2–3) in dissolution rate will be observed above and below the saturation horizon of adjacent sites that receive similar organic carbon inputs.

More recently, benthic flux chamber measurements (Jahnke et al., 1994) have suggested that low metabolic dissolution efficiencies occur at some locations. Also, recent interpretations of fine-scale pore water O_2 distributions have achieved the best fit to the data with a multi-G model (Hales and Emerson, 1996, 1997a). Incorporation of this kinetic description of remineralization into $CaCO_3$ dissolution models reduces the metabolic dissolution efficiency by roughly a factor of 2 to 3 from the early models (Hales and Emerson, 1996, 1997a). Less efficient metabolic dissolution would imply generally less dissolution above the saturation horizon and stronger variations in dissolution rates across the saturation horizon.

Here we present the results from in situ benthic flux chamber incubations on the Cape Verde Plateau and Ceara Rise. Replicate deployments and comparison to previous measurements demonstrate the reproducibility of individual chamber results and corroborate our earlier observation that at selected locations the titration alkalinity (TA) and Ca^{2+} benthic fluxes and inferred efficiency of metabolic dissolution are significantly reduced from the early predictions. The estimated fluxes are then interpreted in the context of our previous results from the California Borderland, central California margin, Ontong Java Plateau and North Carolina continental margin. We propose that the depression of metabolic dissolution efficiency observed at high $CaCO_3$, supersaturated sites can be explained by precipitation of $CaCO_3$ at the sediment surface. A numerical simulation is presented to demonstrate the feasibility of this explanation. Additionally, surface exchange reactions coupled

Table 1. Summary of expedition dates, locations, and water depths.

Date/ship	Deployment designation	Water depth (m)	Sample ID	Latitude (°N)	Longitude (°W)
Jan 1991	Cape Verde				
R/V L'Atalante	bcj-2	3120	CV1	18 27.76	21 01.51
	bcj-3	3105	CV2	18 30.15	21 03.60
Nov 1998	Cape Verde				
R/V Knorr	bfc-87	3103	CV3	18 27.86	21 01.48
	bfc-91	3102	CV4	18 28.01	21 01.54
Mar 1994	Ceara Rise				
R/V Knorr	A1	3995	CR1	05 17.01	43 33.06
	B8	3272	CR2	05 15.09	44 08.16
	G40	4675	CR3	06 09.33	42 52.02
	G69	4677	CR4	06 09.40	42 52.25

with high sediment mixing rates may also act to depress metabolic dissolution at these high-$CaCO_3$ locations.

2. METHODS

2.1. Study Regions

In situ benthic flux chamber results are reported here from two deep sea areas within the North Atlantic, the Ceara Rise and the Cape Verde Plateau. The results are then compared to previously published results from four other regions also shown in Figure 1. Specific locations and cruise designations for the results reported here are listed in Table 1; selected bottom water and sediment characteristics for these regions are listed in Table 2. Water depths for the individual stations range from 3102 to 4676 m. Over this depth range, bottom waters at all but the deepest site at the Ceara Rise (CR3 and 4) are supersaturated with respect to calcite. Bottom water O_2 concentrations at all of these sites are $>$ 200 μmol kg^{-1}. Significant differences are observed in the $CaCO_3$ content of the sediments among the sites. On the Cape Verde Plateau and above the saturation horizon on the Ceara Rise, sediments are dominated by $CaCO_3$, ~65% by weight. Below the saturation horizon on the Ceara Rise, lower $CaCO_3$ contents are measured (Curry and Lohmann, 1990). Note that oxygen, titration alkalinity and calcium fluxes for Cape Verde stations CV1 and 2 were previously published (Jahnke et al., 1994).

2.2. Field Methods

At the locations indicated in Table 2, in situ benthic flux incubations were performed with the free vehicle instrument described in Jahnke and Christiansen (1989). This device is an autonomous instrument that implants a single 30 $\times$ 30 cm titanium chamber into the surface sediment upon deployment. After a preset time period, an hydraulic system closes a lid over the chamber and an inert tracer (NaBr) is injected into the chamber water so that the chamber volume can be determined and the seal of the lid verified. Rotating rods gently stir the enclosed water at a rate determined previously to maintain a 300 to 500 μm thick diffusive sublayer (Buchholtz–ten Brink et al., 1989). At preset time intervals, a total of eighteen samples of the chamber waters are collected, half into plastic medical syringes and half into glass ampules (oxygen samples only). At the end of the experiment, an hydraulic system is activated to close a scoop under the chamber to capture the sediments, expendable weights are released and the instrument returns to the surface for recovery.

In response to earlier measurements on the Cape Verde Plateau and Ontong Java Plateau that yielded lower than expected TA and Ca^{2+} fluxes (Jahnke et al., 1994), it had been suggested that there may be an unidentified alkalinity sink within the titanium chambers that were initially used (Hales, 1995). Although such an artifact would not affect the Ca^{2+} results which were consistent with the earlier TA results, it was still argued that this would reduce the observed alkalinity flux, masking the true rate of metabolic $CaCO_3$ dissolution. Because the concentration changes in Ca^{2+} and TA are so small during the deep sea incubations, a small blank would correspond to a significant uncertainty in the flux. Reproducing deep sea floor conditions, including deep sea pressures, precisely enough in the laboratory to test for such losses with the required precision was considered not possible. Therefore, to test whether the lower than expected TA fluxes were due to consumption associated with the titanium chamber, the titanium chamber on one of the instruments was replaced with a 30-cm-diameter chamber constructed from PVC. In this chamber, stirring of the chamber waters was provided by a SeaBird impeller pump. Recent simulation models demonstrate that for deployments $>$ 10 h in duration benthic O_2 fluxes, and presumably metabolic CO_2 production, are not sensitive to two-fold variations in diffusive sublayer thickness (Reimers et al., 2001). The results with this different stirring scheme should still be comparable to the earlier results and provide a test of the accuracy of the titanium chamber results.

2.3. Analytical Methods

Once the free vehicle instrument was recovered, the O_2 samples were immediately fixed in the glass ampules using the reagents prescribed for Winkler titrations (Strickland and Parsons, 1972; scaled to the volume of the ampules, ~11 mL) and the plastic syringe samples were filtered through 0.45-μm-pore-diameter Gelman HT Tuffryn membrane filters. Sample pH was measured by glass electrode calibrated with NIST-traceable buffers and the samples were stored refrigerated until analysis. Samples were analyzed for $Si(OH)_4$, PO_4^{3-} and NH^{4+} using scaled-down colorimetric methods of Strickland and Parsons (1972) to a precision of $\pm$2%. Nitrate + nitrite concentrations were determined manually for CV 1 and 2 by a scaled-down version of the method of Strickland and Parsons (1972) and using an Alpkem autoanalyzer for CV 3 and 4 and CR 1 to 4, also to an analytical precision of $\pm$2%. TA was measured by Gran titration (precision $\pm$0.5%). Bromide concentrations were determined by the method of Morris and Riley (1966) to $\pm$5%. Calcium concentrations were determined by the EGTA titration method adapted from Tsunogai (1968). Because sample volume and most of the titrant volume were determined by weight, an analytical precision of better than $\pm$0.05% was achieved. All constituent concentrations from each chamber sample were measured in duplicate aliquots, except for Ca^{2+} and TA, which were measured in triplicate or quadruplicate aliquots.

Table 2. Selected bottom water characteristics of the study regions. Ceara Rise saturation states were taken from Hales and Emerson (1997a).

	Parameter					
Location	Water depth (m)	Oxygen (μmol/L)	Nitrate (μmol/L)	IAP/K_{sp}	ΔCO_3^{2-}	Sedimentary $CaCO_3$ (wt%)
Ceara Rise 1	3995	263	20.3	1.02	+2	63
Ceara Rise 2	3272	261	20.1	1.23	+24	65
Ceara Rise 3–4	4676	232	25.0	0.78	–19	35
Cape Verde	3103	242	20.4	1.26	+33	65

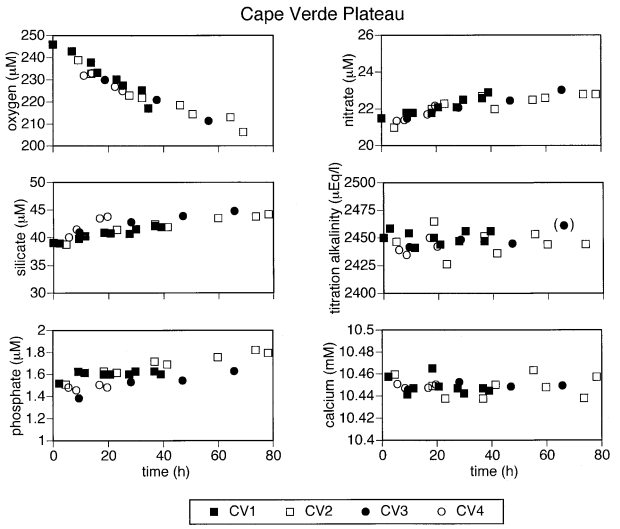

Fig. 2. Benthic flux chamber results from four independent deployments on the Cape Verde Plateau: two deployments from January 1991 (CV1 and CV2) and two deployments from November 1998 (CV3 and CV4).

3. RESULTS

3.1. Determination of Chamber Volume and Benthic Fluxes

Benthic flux chamber results from the Cape Verde Plateau and Ceara Rise are presented in Figures 2 and 3. For the Cape Verde Plateau, the previously-published results obtained in January 1991 are plotted along with the more recent results for comparison. Note that deployment CV4 employed a PVC chamber. Additional PVC-Ti chamber comparisons have already been reported from the Western Atlantic (Jahnke and Jahnke, 2000) and are discussed later. Below the saturation horizon at the Ceara Rise, two successive independent deployments were performed (Fig. 3C) and these are also presented together for comparison.

Except for the solutes discussed in detail below, most of the results are qualitatively similar at all of the study sites. Oxygen decreases with incubation time in the chamber due to utilization by benthic organisms and possibly inorganic chemical reactions such as sulfide oxidation. Similarly, NO_3^-, PO_4^{3-} and $Si(OH)_4$ concentrations increase within the chambers due to remineralization and oxidation of organic matter and dissolution of opal in the surface sediments. Titration alkalinity and Ca^{2+} results are more variable and will be discussed in detail in a following section.

The effective volume of chamber water for each deployment was estimated from the observed dilution of the tracer injected at the beginning of the incubation. Due to initial concerns about potential contamination, a tracer was not employed in the 1991 deployments (CV1 and 2) and chamber volume was estimated by direct measurement of water column height within the retrieved core. The amount of tracer injected is known from the syringe volume and concentration of the stock solution (46 mL volume and 0.6 mol/L NaBr for CR1–4; 46 mL volume and 0.3 mol/L NaBr for CV3 and 4, respectively). The concentration of Br^- in the chamber waters in excess of that which is naturally present in sea water (ex Br^-) at the start of the incubation was estimated by extrapolation of the time series results to the start of the incubation by linear regression. Excess Br^- concentrations generally decreased linearly with incubation time (Fig. 4). The rapid rate of decrease measured in deployment CV4 is indicative of enhanced pore water - bottom water exchange most likely due to irrigation activities of macrobenthic organisms. This exchange may account for the large NO_3^- and $Si(OH)_4$ fluxes estimated for this deployment as discussed below. Because the cross-sectional area of the chamber is known, the chamber height could be estimated. A linear regression of the concentration time-series results was calculated and the benthic flux was then estimated by multiplying the slope of the regression by the effective chamber height. Subsequent modeling efforts by Rao and Jahnke (2002) have shown that in cases with substantial pore water irrigation rates, linear extrapolation can significantly overestimate chamber volumes. For the flux results reported here, differences in the two techniques are generally significantly $< 10\%$ and are ignored. More importantly, the main discussion presented here is based on flux ratios which are completely independent of chamber volume estimates. The flux estimates for all deployments are listed in Table 3. The uncertainty represents one standard error of the regression slope.

3.2. Cape Verde

At the Cape Verde Plateau, a large and consistent decrease in chamber O_2 is measured in all deployments (Table 3), yielding flux estimates that range from -0.67 to -1.02 mol m^{-2} yr^{-1}. Using the measured O_2 flux and assuming Redfield (Redfield et al., 1963) stoichiometry (16:138), the expected total nitrogen remineralization rate in the sediments is estimated (Table 4). Assuming no other losses and complete oxidation to NO_3^-, this rate should equal the observed benthic NO_3^- flux; differences would be attributed to remineralization of organic matter that is depleted in N relative to Redfield or to denitrification. Regional deep sediment traps give a N:C ratio of $0.113 \pm 7.3\%$ (Antia et al., in press), suggesting some N depletion in the particulate flux to the sediments in the Cape Verde region. Rates of denitrification required to account for the missing N flux are calculated using both Redfield (N:C 16:106) ratio and the depleted (N:C 12:106) ratio indicated above (Antia et al., in press). The majority of the benthic NO_3^- flux deficit for this region is most likely due to denitrification, as the depleted-N particulate flux does not account for the benthic N flux missing in CV1 to 3. Note that the inferred denitrification rate is small relative to the total remineralization rate in these sediments and does not comprise a significant uncertainty in estimates of metabolic CO_2 production (Table 4).

Phosphate fluxes on the Cape Verde Plateau range from 1.8 to 5.5 mmol m^{-2} yr^{-1} (Table 3). Relative to the estimated C remineralization rate listed in Table 4, this implies a P:C remineralization ratio which ranges from approximately Redfield (0.01) to 0.0023. Silicate fluxes range from 0.083 to 0.345 mol m^{-2} yr^{-1}. For $Si(OH)_4$ there is a very large disparity between CV4, which had a strong pore water irrigation signal, and the other deployments. This is apparent in the absolute flux rates and the estimated Si:C ratio as well. While a very high

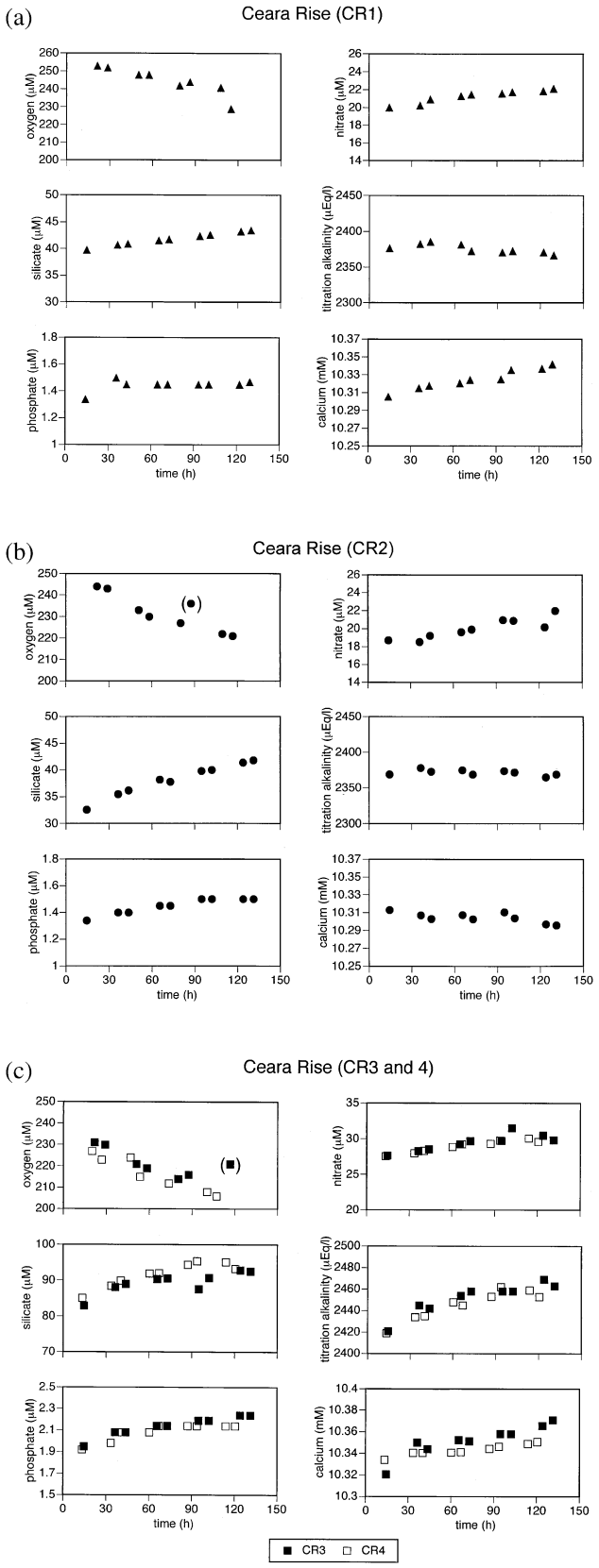

Fig. 3. Benthic flux chamber results from the Ceara Rise above the saturation horizon, stations A (A) and B (B) and from duplicate deployments at station (G) below the saturation horizon (C).

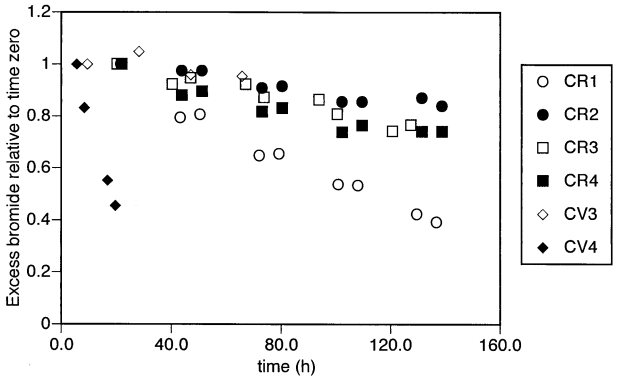

Fig. 4. Excess Br^- results from each chamber deployment normalized to the first sample.

Si:C ratio is estimated for CV4, the ratios estimated for the other deployments are close to the value of 0.13 which is the mean ratio reported for 27 species of pelagic diatoms (Brzezinski, 1985). Deposition and remineralization of organic carbon associated with calcareous species would lower the estimated Si:C sedimentary ratio. Thus despite the high $CaCO_3$ content of the sediments, deposition of organic matter associated with siliceous organisms most probably also contributes significantly to the total organic carbon rain rate.

Although large O_2 fluxes are observed on the Cape Verde Plateau, TA and Ca^{2+} fluxes are near zero (Table 3). The precision of the earlier measurements is lower than for the more recent deployments as our methodology improved, but nevertheless, the results from all of the deployments are consistent.

3.3. Ceara Rise

On the Ceara Rise, O_2 fluxes range from -0.16 to -0.20 mol m^{-2} yr^{-1}. Again, using these fluxes and assuming Redfield stoichiometry, the total organic carbon oxidation rate and nitrogen regeneration rate in the sediments can be estimated (Table 4). Here, the measured NO_3^- fluxes are relatively close to the estimated N regeneration rates, implying that the deposited organic matter is close to Redfield composition and that there is little loss of N via denitrification or that N is preferentially released from N-depleted organic matter at a rate that fortuitously is near the Redfield ratio. Relative uncertainties in the N fluxes are high due to the low absolute fluxes and therefore preclude any further interpretation.

Phosphate fluxes range from 0.5 to 1.5 mmol m^{-2} yr^{-1}. At CR2, 3 and 4, these fluxes are relatively consistent with Redfield whereas at CR1, the remineralization of a P-depleted organic matter is implied. Silicate fluxes range from 0.031 to 0.058 mol m^{-2} yr^{-1} which, when compared to the estimated carbon oxidation rate, imply high Si:C ratios (0.2–0.48). These ratios exceed the reported average for pelagic diatoms of 0.13 (Brzezinski, 1985). One explanation would be the deposition of re-worked organic materials that had preferentially already lost a significant portion of the organic carbon, raising the Si:C ratio. This explanation is, however, inconsistent with the N and P results which implied near Redfield composition for the majority of the sites.

TA and Ca^{2+} fluxes at the Ceara Rise sites are variable. At

Table 3. Summary of in situ benthic chamber flux estimates. Fluxes are in mol m^{-2} y^{-1} ± SE except for TA which is in Eq m^{-2} y^{-1}.

Sample ID	Oxygen	TA	Calcium	Nitrate	Phosphate	Silicate
CV1	–1.020 ± .088	–.010 ± .193	–.277 ± .278	.039 ± .006	.0018 ± .0010	.100 ± .013
CV2	–0.672 ± .063	–.061 ± .210	–.001 ± .190	.025 ± .007	.0050 ± .0005	.083 ± .012
CV3	–0.678 ± .011	.067 ± .084	.052 ± .108	.037 ± .002	.0055 ± .0012	.092 ± .011
CV4	–0.747 ± .153	.110 ± .376	–.018 ± .286	.071 ± .020	.0020 ± .0020	.345 ± .047
CR1	–0.204 ± .037	–.129 ± .039	.289 ± .025	.018 ± .002	.0005 ± .0004	.031 ± .005
CR2	–0.169 ± .035	–.034 ± .025	–.079 ± .028	.019 ± .004	.0011 ± .0002	.056 ± .004
CR3	–0.159 ± .020	.236 ± .040	.092 ± .010	.016 ± .002	.0013 ± .0003	.058 ± .013
CR4	–0.181 ± .025	.224 ± .039	.227 ± .039	.017 ± .004	.0015 ± .0001	.043 ± .012

CR1 and 2 which are above the saturation horizon, no TA flux out of the sediments is measured within the analytical uncertainty of the measurement. In fact, at CR1 a small but consistent flux into the sediment is observed. As discussed later, this could be due to a small net precipitation of $CaCO_3$ at the sea floor. Below the saturation horizon at CR3 and 4, a steady and consistent flux out of the sediments is observed. Thus, independent of the absolute flux rates which will be discussed in detail later, there is a clear difference in TA fluxes between sites above and below the saturation horizon even though the O_2 flux and presumed metabolic CO_2 production rates are similar. This is in contrast to the dissolution rates estimated from pore water gradients by Martin and Sayles (1996) but is qualitatively consistent with sedimentological evidence discussed in Broecker and Clark (2003).

With the exception of CR1, Ca^{2+} fluxes follow the TA fluxes. Consistent and readily detectable fluxes are observed for both deployments at the undersaturated site (CR3 and 4), and no flux out of the sediments is observed at CR2. At CR1, a large Ca^{2+} flux out of the sediments is observed without a corresponding TA flux. This is discussed in greater detail in the "Discussion" section.

The results presented here are in agreement with earlier benthic flux chamber results that suggested significant regional variations in benthic TA flux relative to the O_2 flux. The challenge is to develop a model that explains the variations observed.

4. DISCUSSION

Our results will be interpreted in the context of our previously reported in situ chamber results from the Cape Verde Plateau, Ontong Java Plateau (Jahnke et al., 1994), California Borderland Basins (Jahnke, 1990), California continental slope and rise (Jahnke et al., 1997) and North Carolina continental slope and rise (Jahnke and Jahnke, 2000).

4.1. Calcium and Titration Alkalinity Fluxes

To test whether TA and Ca^{2+} distributions are primarily controlled by the dissolution of $CaCO_3$, the measured Ca^{2+} flux is plotted against 1/2 of the TA flux in Figure 5. The majority of the results follow the 1:1 line reasonably well, suggesting that at these sites, Ca^{2+} and TA fluxes are controlled by the dissolution or precipitation of $CaCO_3$. However, inexplicably high Ca^{2+} fluxes (relative to the TA flux) at the four sites within the North Carolina slope depocenter (Sites B, E, H, and I from Jahnke and Jahnke, 2000) are observed and were noted previously. These sites are extremely reducing and the high Ca^{2+} fluxes may be caused by the formation of carbonate solid phases that are enriched in Mg^{2+} relative to the initially deposited carbonates, resulting in a Ca^{2+} flux that is larger relative to the TA flux. There is no direct evidence at present to support this possible explanation.

An anomalously high Ca^{2+}:TA flux ratio is also observed at CR1 on the Ceara Rise. Given the analytical challenge of quantifying small Ca^{2+} fluxes against a large sea water background concentration, some scatter around the 1:1 line in Figure 5 is expected. However, this is the only deployment from stations deeper than 1000 m where the Ca^{2+} and TA fluxes are statistically different from the expected relationship. Perhaps at this site, other Ca^{2+}-containing phases, supplied tectonically, are dissolving and contributing to the Ca^{2+} flux. It is important

Table 4. Summary of measured and calculated nutrient fluxes.

Sample ID	O_2 flux (mol/m^2 yr)	CO_2 produced (mol/m^2 yr) (assumes 106:138)	N expected[a] (mol/m^2 yr)	N measured (mol/m^2 yr)	Denitrification[a] (mol/m^2 yr)	% denitrified[a]	P flux (mol/m^2 yr)	P:C regenerated	Si flux (mol/m^2 yr)	Si:C regenerated
CV1	–1.020	0.783	0.089–0.118	0.039	0.050–0.079	56–67	0.0018	0.0023	0.100	0.128
CV2	–0.672	0.516	0.058–0.078	0.025	0.033–0.053	57–68	0.0050	0.0097	0.083	0.161
CV3	–0.678	0.521	0.059–0.079	0.037	0.022–0.042	37–53	0.0055	0.0106	0.092	0.177
CV4	–0.747	0.574	0.065–0.087	0.071	–0.006–0.016	−10–18	0.0020	0.0035	0.345	0.601
CR1	–0.204	0.157	0.024	0.018	0.006	24	0.0005	0.0032	0.031	0.198
CR2	–0.169	0.130	0.020	0.019	0.001	3	0.0011	0.0085	0.056	0.431
CR3	–0.159	0.122	0.018	0.016	0.002	13	0.0013	0.0106	0.058	0.475
CR4	–0.181	0.139	0.021	0.017	0.004	19	0.0015	0.0108	0.043	0.309

[a] Calculated for Cape Verde location as a range based on Redfield N:C of 16:106 and on N:C measured from regional sediment traps of 12:106 (Antia et al, in press).

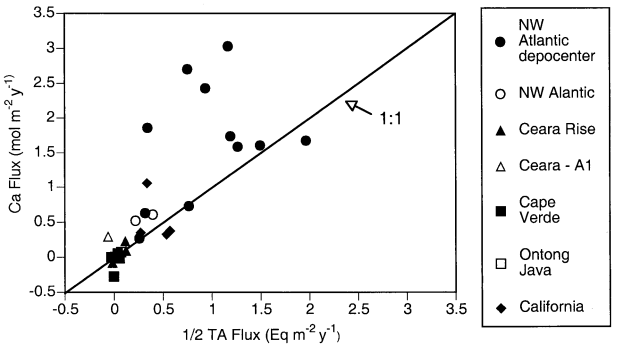

Fig. 5. Titration alkalinity flux vs. Ca^{2+} flux for all flux chamber results.

to point out that the $\delta^{13}C$ results for this deployment are also anomalous in that no change in $\delta^{13}C$ is observed in the chamber waters (D. McCorkle, personal communication). On face value, this would suggest that the oxidation of organic carbon does not contribute to the TCO_2 flux despite a measurable O_2 flux. This result is also contrary to all previous benthic flux chamber observations and modeling results (Gehlen et al., 1999) and suggests that processes other than diagenesis of organic matter and $CaCO_3$ are contributing to the fluxes of Ca^{2+} and carbonate system species at this site. Since our purpose here is to examine the relationship between remineralization and $CaCO_3$ dissolution, the results from this deployment must be cautiously interpreted.

Despite these anomalous observations, we conclude that at virtually all of the deep sea benthic flux chamber sites, TA fluxes and Ca^{2+} fluxes are well correlated. Furthermore, within the analytical uncertainties, the TA flux is twice the Ca^{2+} flux, suggesting that the dissolution/precipitation of $CaCO_3$ is the primary control of the benthic TA flux. In the following, we will use TA flux as a measure of $CaCO_3$ dissolution.

4.2. Regional Variations in Titration Alkalinity Chamber Results

We first compare the results reported here with all of our previously reported benthic flux results (Fig. 6). The results are reported as the ratio of 1/2 of the benthic TA flux to the organic carbon remineralization rate. The latter is estimated as 0.77 (the Redfield C:O_2 ratio) times the measured benthic oxygen flux. At two locations in the Santa Monica Basin where O_2 fluxes were not available, the remineralization rate was estimated by subtracting 1/2 of the TA flux from the measured TIC flux.

To help identify the trends, we have grouped the results in Figure 6 into four categories: supersaturated bottom waters with high and low sedimentary $CaCO_3$ and undersaturated bottom waters with high and low sedimentary $CaCO_3$. For the supersaturated sites, high $CaCO_3$ sites contain $>$ 60% by weight $CaCO_3$ while low carbonate sites contain $<$ 5% $CaCO_3$.

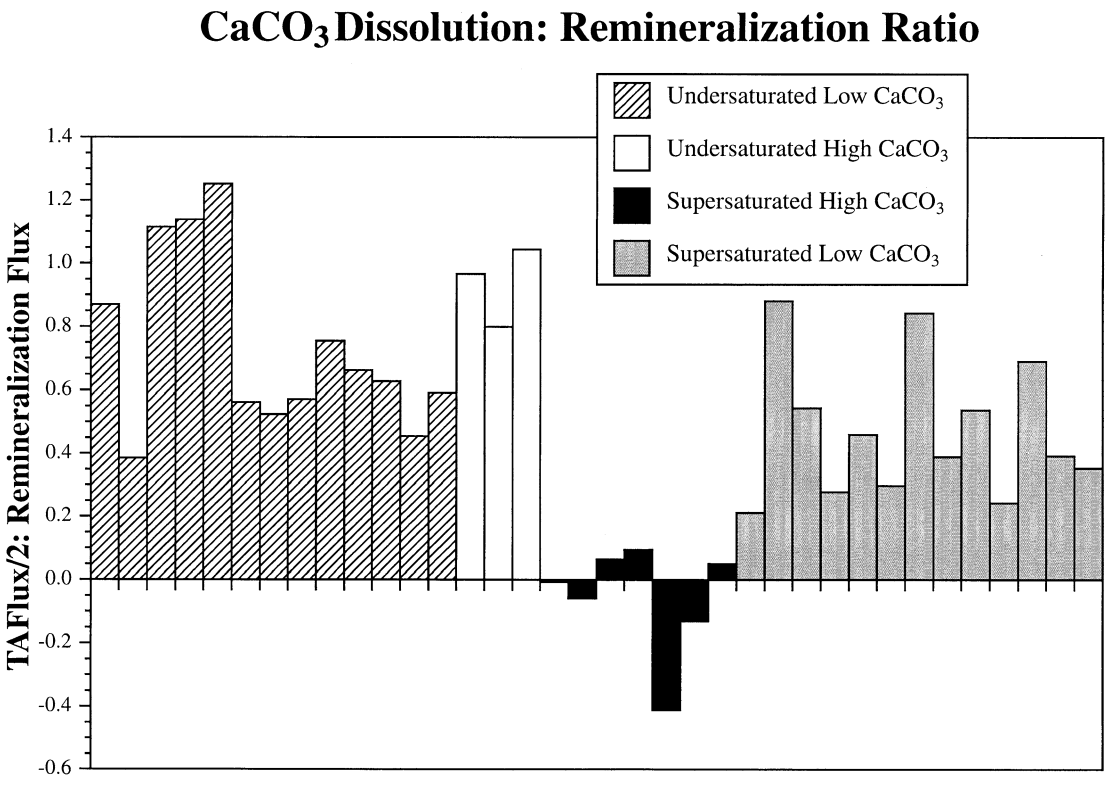

Fig. 6. Summary of the ratio of TA or Ca^{2+} benthic flux to the organic carbon remineralization rate for deployments from the Northeastern Pacific, Ontong Java Plateau, Ceara Rise, Cape Verde Plateau, North Western Atlantic continental rise and California Borderland Basins.

Table 5. Mean ratios of $CaCO_3$ dissolution rate to organic carbon oxidation rate for the indicated sea floor conditions.

Undersaturated, Low $CaCO_3$	Undersaturated, High $CaCO_3$	Supersaturated, High $CaCO_3$	Supersaturated, Low $CaCO_3$
0.73 ± 0.28	0.94 ± 0.27	-0.077 ± 0.18 (0.002 ± 0.08 less CR1)	0.47 ± 0.22

The average ratio for each category is listed in Table 5. The ratio from incubations at sites with undersaturated bottom waters displayed only minor differences between high (>35%) and low (<5%) $CaCO_3$ sites. At undersaturated, high-carbonate sites, the ratio ranged from 0.8 to 1.04 with an average value of 0.94. These ratios are qualitatively similar to those estimated from O_2 and TA fluxes reported by Berelson et al. (1990) for the central equatorial Pacific (MANOP Site C). At undersaturated, low-$CaCO_3$ sites, values ranged from 0.39 to 1.25 with an average value of 0.73. Of course, both inorganic and metabolic dissolution can be contributing to the TA flux at these sites. Furthermore, at sites where sedimentary $CaCO_3$ is extremely low, dissolution would become limited by $CaCO_3$ availability and very low ratios would be expected. These factors may explain some of the variability observed.

In contrast, extremely large differences are observed between the high and low $CaCO_3$ sites when the bottom waters are supersaturated. Where sedimentary $CaCO_3$ is low, values range from 0.21 to 0.88 with an average value of 0.47. It is important to also note that within this group, the deployments represented by the last 6 bars in this histogram employed PVC chambers while the first 7 bars are based on results from Ti chambers (Fig. 6). Average ratios for the Ti and PVC chambers were 0.50 and 0.44, respectively, which is not considered significantly different in this context. There appears to be no influence of chamber material at these supersaturated sites. Where sedimentary $CaCO_3$ is high, however, ratios range from < 0 to 0.1 with an average value of -0.08. If the value from the anomalous CR1 on the Ceara Rise is omitted, a mean value for the other deployments of 0.002 is obtained. As discussed previously, the results from CR1 on the Ceara Rise are anomalous and our best guess for the relevant mean value for this group of deployments is essentially zero. The low ratio values observed at these high-$CaCO_3$, supersaturated stations are obvious in Figure 6. It is important to recognize that these low ratios were obtained on 7 completely independent deployments over a 7-yr period, at three widely separate locations (Cape Verde Plateau in 1991 and 1998, Ceara Rise in 1994 and the Ontong Java Plateau in 1991) using chambers that were constructed from titanium or PVC. It appears that the depression of TA and Ca^{2+} benthic fluxes at high-$CaCO_3$, supersaturated sites is a robust observation.

Qualitatively, except for the supersaturated, high-$CaCO_3$ case, the differences among the mean ratios listed in Table 5 for the different conditions follow our present understanding of sediment diagenesis. Undersaturated conditions allow for inorganic and metabolic dissolution and one would expect the greatest dissolution rates where the $CaCO_3$ content is highest. This is consistent with the higher ratio measured at the high-$CaCO_3$ sites. Under supersaturated conditions, inorganic dissolution is eliminated and, relative to carbon oxidation rates, one would expect TA/2:remineralization ratios to be reduced. At low-$CaCO_3$ sites this is observed, where the mean ratio is lower in supersaturated conditions relative to undersaturated conditions. For the supersaturated sites, one would expect a higher ratio at high-$CaCO_3$ sites because metabolic CO_2 would have a larger $CaCO_3$ pool to react with. Instead, very low to near zero flux ratios are measured. Clearly, expected TA and Ca^{2+} benthic flux rates are not observed in chambers at the supersaturated, high-$CaCO_3$ sites and the following discussion focuses on these results.

As discussed in numerous previous publications, many factors may control the extent or efficiency of metabolic dissolution. The most frequently discussed factors include the dissolution kinetics of the $CaCO_3$ minerals and the organic carbon oxidation profiles in sediments. While it is easy to envision sea floor situations where variations in these factors would lead to variability in the extent of metabolic dissolution, it is more difficult to envision why variations in these factors would be correlated with high sedimentary $CaCO_3$ over the wide geographic ranges reported here.

One might expect metabolic CO_2 production to be shallower or deeper in the sediments if the lability of the organic matter raining to the sea floor varied, resulting in variations in metabolic dissolution efficiency. However, the three sites where low TA fluxes were observed include the Cape Verde Plateau, which is adjacent to the west African coastal upwelling region and experiences substantial fresh organic carbon inputs, and the Ceara Rise and Ontong Java Plateau, which are in the western equatorial Atlantic and Pacific Oceans, respectively, with low organic carbon inputs. Similarly, because this pattern is consistent among the six, widely distributed areas studied, it is unlikely that $CaCO_3$-precipitating species differences and compositional differences within the biogenic $CaCO_3$ materials can cause these patterns.

In the following sections, we advance two basic hypotheses that may explain our observations. In the first section, we hypothesize that inorganic precipitation of $CaCO_3$ at the supersaturated sediment surface followed by dissolution in the undersaturated deeper pore waters may provide an explanation. A quantitative numerical model is presented to demonstrate this possibility. In the second section, the potential impact of surface exchange reactions coupled with sediment mixing is discussed. While we are not yet in a position to test this explanation quantitatively, simple calculations are presented to demonstrate this possibility. It is important to recognize at this point that both of these processes could contribute to the overall observed flux patterns.

4.3. $CaCO_3$ Precipitation

To investigate the potential role of precipitation in altering the benthic fluxes and pore water distributions, the diagentic model previously described in Jahnke et al. (1982, 1994, 1997) and Jahnke (1998) was modified to include a first order precipitation term expressed as

$$\text{Precipitation rate} = k_{ppt} S_{cal} (\Omega - 1)$$

where k_{ppt} is a first-order rate constant, S_{cal} is the $CaCO_3$ content of the sediments and Ω is the ratio of the ion activity

product to the solubility constant. The transport processes simulated in this model include sediment burial, expressed as the advection of particles downward, away from the sediment water interface; particle mixing, represented by a biodiffusion coefficient; and solute transport, described as molecular diffusion through the pore waters. The sediment porosity is assumed to decrease exponentially from a value of 0.9 at the sediment surface to 0.7 at 10 cm. Effective pore water diffusion coefficients were estimated as $D_s = \Phi^2 D_m$, where D_s is the effective diffusion coefficient in the pore waters, D_m is the molecular diffusion coefficient and Φ is the porosity (Ullman and Aller, 1982). In keeping with recent publications (Hales and Emerson, 1997b), we have also assumed that $CaCO_3$ dissolution can be described as a first-order reaction relative to pore water saturation and not a higher-order expression as is often used. Our conclusions are not sensitive to this assumption.

An example of the model results is provided in Figure 7. Four different calculations are presented; that of no precipitation and three cases where the precipitation rate constant is progressively increased as indicated. The bottom water characteristics, particulate flux values and rate constants used in the calculation are listed in Table 6. Our purpose here is to demonstrate that under reasonable deep ocean conditions, a diagenetic model that includes precipitation can provide an explanation for the observed results. We have therefore set the bottom water oxygen concentration and rain rate of organic carbon to values similar to those encountered on the Ceara Rise but have not attempted to obtain a best fit for any specific location. We have set the bulk sediment accumulation rate and sediment mixing rate to values that are reasonable but generally higher than encountered in most low rain rate deep sea locations. Also, we have used a relatively slow organic carbon degradation rate. The combination of faster accumulation and mixing and slower degradation enhances the efficiency of metabolic dissolution and thereby provides a robust test of the precipitation hypothesis. Indeed, for the "no precipitation" case presented in Figure 7, 67% of the metabolically released CO_2 is neutralized by the dissolution of $CaCO_3$.

For all model runs, the O_2 benthic chamber flux and pore water distribution are essentially identical. While altering the precipitation rate also alters preservation of $CaCO_3$ and the total sediment accumulation, the impacts of these changes are negligible on the pore water O_2 profiles. Large changes are observed in the simulated carbonate alkalinity (CA) chamber fluxes (and Ca^{2+} benthic fluxes—results not shown but proportional to the CA results). As the precipitation rate constant is increased, fluxes decrease to essentially zero at the highest rate simulated. Below a few millimeters, the pore water CA profile remains relatively constant. Within the upper 2 mm, however, increasing rates of $CaCO_3$ precipitation draw the pore water CA to progressively lower values, forming a minimum at the highest rates. This minimum is a consequence of the fact that the CA flux is the sum of the HCO_3^- and $2CO_3^{2-}$ fluxes which are of opposite sign and that the molecular diffusion coefficients for these two solutes differ. It is important to note that this minimum in TA occurs when there is no net interfacial flux of TA as shown by the simulated chamber results for CA. The TCO_2 flux decreases somewhat as precipitation increases but not as dramatically as CA decreases because the majority of the TCO_2 is supplied by remineralization of organic carbon.

As precipitation is increased, the pH and saturation state gradients in the upper few millimeters decrease more sharply with sediment depth. Thus, this system is somewhat self regulating in that as the rate of precipitation increases, the thickness of the supersaturated layer at the surface decreases. Finally, it is observed that as the rate of precipitation is increased, the preservation of $CaCO_3$ increases. When the CA benthic flux is essentially zero, $CaCO_3$ is buried at its input value of 80%.

Several other aspects of this potential explanation should be noted. First, precipitation at the rate employed to mask metabolic dissolution is sufficiently slow that it would not significantly alter water column distributions or oceanic mass balances. If a particle takes 2 weeks to sink through a hypothetical water column that is 3× supersaturated with respect to $CaCO_3$, the mass of $CaCO_3$ contained in the particle would increase by only 3% at the highest precipitation rate employed here. More importantly, because the molar ratio of organic carbon to $CaCO_3$ in raining particulate matter is close to one, this inorganically-precipitated $CaCO_3$ would most likely be redissolved at the sea floor due to metabolic dissolution. Thus, unless total precipitation rates exceed that which can be redissolved by metabolic dissolution, global balances remain unchanged. Second, because particle mixing will transport particles into and out of the thin, supersaturated surface layer many times during transit through the mixed layer, a very small standing stock of this freshly precipitated $CaCO_3$ is required to neutralize the rate of metabolic CO_2 production. This is evident in the model results by the absence of a large difference in the $CaCO_3$ content of the sediments between the surface, supersaturated layer and the deeper, undersaturated zone.

Finally, Martin et al. (2000) have estimated the ^{14}C activity of the carbon released by $CaCO_3$ dissolution at locations above and below the saturation horizon on the Ceara Rise. Below the saturation horizon, dissolution appeared to supply carbon that was isotopically younger (perhaps containing bomb ^{14}C) while at the site above the saturation horizon old carbonate appeared to be dissolving. This is consistent with the precipitation hypothesis. Below the saturation horizon, the sediments are always undersaturated and dissolution releases carbonate dominantly (except for the potential dissolution of a small amount of benthic foram material) supplied from surface water production. This yields young ages. Above the saturation horizon, the sediment surface is supersaturated and $CaCO_3$ may be precipitating from bottom waters which contain relatively old carbonate. When this material re-dissolves due to metabolic dissolution, old carbonate is released to the pore waters.

Thus, precipitation of $CaCO_3$ at sites that are overlain by supersaturated bottom waters and that contain sufficient $CaCO_3$ to act as nucleating surfaces appears to provide a feasible explanation for the in situ benthic chamber, in situ microelectrode, pore water and solid phase results.

4.4. Adsorption/Desorption/Mixing

While the above precipitation mechanism provides an attractive explanation for our results, other factors may also influence metabolic dissolution efficiency. Van Cappellen et al. (1993) developed a model of surface hydration species for the carbonate mineral surface in aqueous solutions containing CO_2 (Table 7). It is clear from the table that these reactions exchange

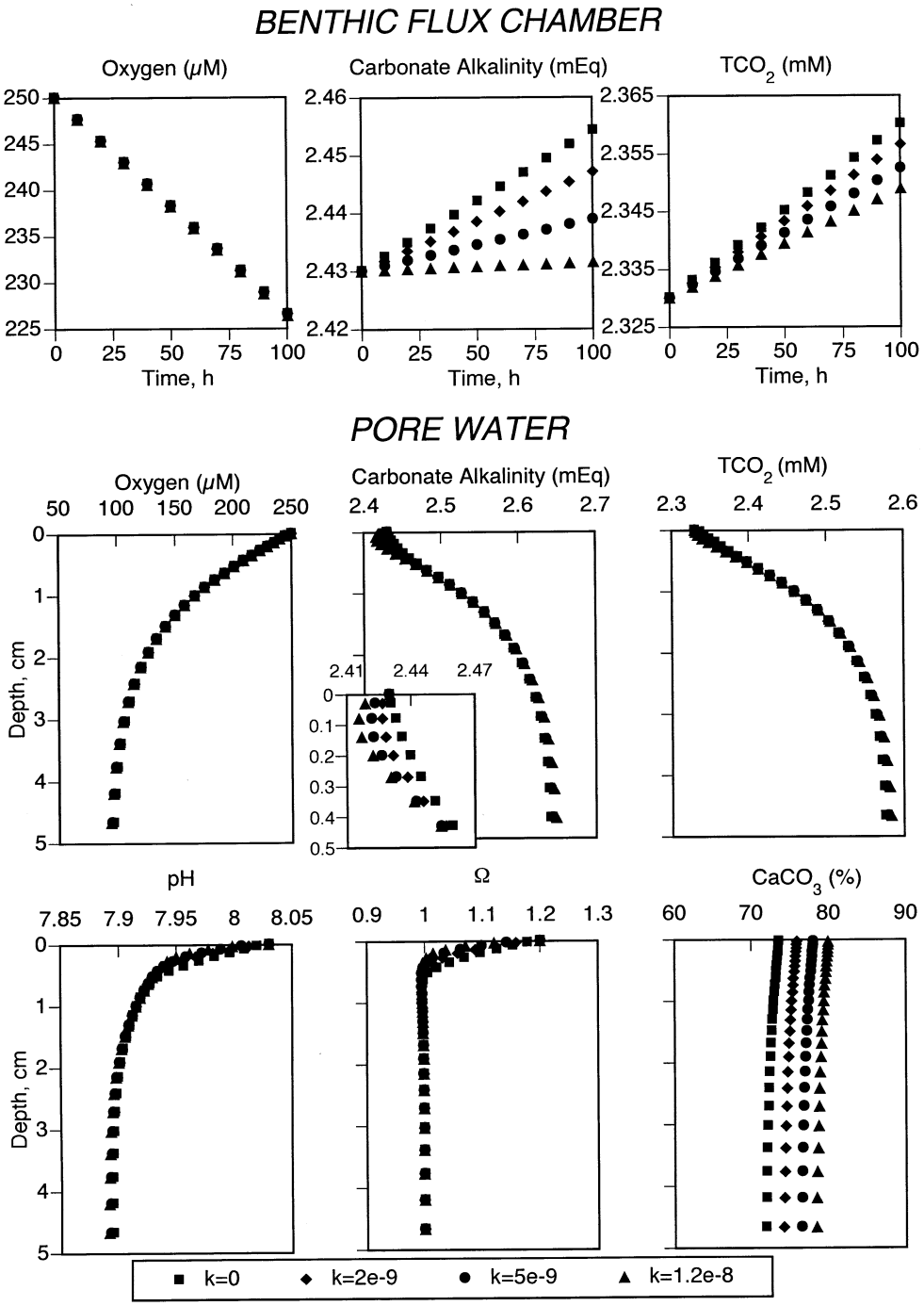

Fig. 7. Summary of benthic fluxes and pore water and sediment distributions obtained by a numerical simulation of sediment diagenesis which includes inorganic $CaCO_3$ precipitation. Rate constants for precipitation are provided at the bottom of the figure.

protons (and hence alkalinity), CO_2 and Ca^{2+} between the pore waters and mineral surface. Thus, if sufficiently abundant, these reactions are capable of influencing carbonate system equilibria.

An accurate chemical model for the hydration and carbonate system and Ca^{2+} exchange processes on the calcite mineral surface in sea water does not presently exist. Nevertheless, a 'back-of-the-envelope' estimate of the potential magnitude of the exchange can be achieved by using the exchange constants reported in van Cappellen et al. (1993) and sea water values of Ca^{2+}, TA and pH (Table 8). Under the conditions given in the Table legend, the distribution of dissolved and surface sorbed species in the sediments is listed per cubic centimeter of wet sediment.

Table 6. Summary of conditions and rate constants employed for the example calculation displayed in Figure 7.

Parameter	Value and comments
Bottom water oxygen conc.	250 μmol/L
Total sediment rain rate	0.55×10^{-10} cm^3 cm^{-2} s^{-1} (at $\Phi = 0.8$, equivalent to 8.7 cm kyr^{-1})
Sediment mixing rate	6×10^{-10} cm$^3_{sed}$ cm^{-1} s^{-1} (at $\Phi = 0.8$, equivalent to 95 cm^2 kyr^{-1})
Carbonate rain rate	0.37 mol $CaCO_3$ m^{-2} yr^{-1}
Organic carbon rain	0.159 mol OC m^{-2} yr^{-1}
Bottom water saturation	1.21
Dissolution rate constant	0.1% d^{-1}
OC degradation rate	0.017% d^{-1}
Diffusive sublayer thickness	0.05 cm

It should be recognized that the distributions listed in Table 8 do not consider the competing ions, such as Mg^{2+}, that would be found in natural sea water. Additionally, the constants used by van Cappellen et al. (1993) were based on solution-phase constants that were adjusted for surface potential. The absolute values, therefore, should be viewed as providing a sense of the magnitude of exchange sites available and not an actual representation of the specific distributions. Even with this caveat in mind, it is clear that per cubic centimeter of wet sediment, exchange sites on the mineral surfaces may greatly outnumber the equivalents of carbonate alkalinity in the associated pore waters. Acid/base exchange reactions with these sites (Table 7) could, therefore, significantly impact the pore water calcite saturation state.

We hypothesize that this high exchange capacity can influence our results in two ways. First, exchange with the mineral surface at the sediment water interface might tend to buffer the chamber waters, minimizing the concentration changes that are observed during the incubation. However, it is important to note that relative to the concentration changes that occur in the chamber waters, pore water concentrations change rapidly with depth. Sediment particles 1 to 2 mm below the sediment surface are in equilibrium with aqueous concentrations that are larger than those observed in the chambers. It is unlikely, therefore, that the surface sediments could buffer chamber concentration changes to the extent required to completely mask the occurrence of metabolic dissolution.

Second, in the presence of a steep gradient in carbonate system parameters, the mixing of particles vertically will augment the diffusive pore water flux because as the particles are translocated from one horizon to another, they will gain or release surface species in response to the new local aqueous conditions. The significance of this transport with respect to sediment diagenesis and metabolic dissolution is determined by the rate of transport due to particle mixing and surface exchange.

It is not possible to explicitly evaluate the rate of solute transport due to surface exchange–particle mixing. As noted before, a mineral surface speciation model does not exist for $CaCO_3$ in sea water; the exchange constants are based on solution constants adjusted by the mineral surface potential and the model does not include competing ions that would be found in sea water such as Mg^{2+}. Furthermore, fine-scale pore water carbonate system gradients have not been evaluated at all benthic flux chamber deployment sites and particle mixing rates over the upper 0.5 to 1.0 cm, where much of the remineralization occurs, are unknown. In the following, we use differences between shipboard and in situ extracted pore water results at high $CaCO_3$ sites (Emerson et al., 1982) to estimate the particle mixing rate required for the surface exchange–particle mixing flux to be equivalent to the pore water alkalinity flux.

Jahnke et al. (1982) reported significant differences in pH, TA and Ca^{2+} values between in situ harpoon and shipboard-extracted pore waters from carbonate-rich, deep sea sediments. While shipboard pH values decreased from in situ values by 0.11 units, TA and Ca^{2+} concentrations decreased by 552 μEq and 920 μmol/L, respectively. Emerson et al. (1982) postulated that these changes were due to the exchange of protons and other carbonate system species with the calcite surface during

Table 7. Carbonate mineral surface exchange reactions identified by van Cappellen et al. (1993).

$$>CO_3H^0 \leftrightarrow >CO_3^- + H^+$$
$$>CO_3H^0 + Ca^{2+} \leftrightarrow >CO_3Ca^+ + H^+$$
$$>CaOH_2^+ \leftrightarrow >CaOH^0 + H^+$$
$$>CaOH^0 \leftrightarrow >CaO^- + H^+$$
$$>CaOH^0 + CO_2 \leftrightarrow >CaCO_3^- + H^+$$
$$>CaOH^0 + CO_2 \leftrightarrow >CaHCO_3^0$$

Table 8. Estimated distribution of pore water and surface carbonate system species in a hypothetical cm^3 of carbonate sediments. Dissociation constants reported by van Cappellen et al. (1993) for the simple $CaCO_3$-CO_2-H_2O system were used. Assumed pore water and sediment conditions are: pw total CO_2 concentration = 2230 μmol/L; pw carbonate alkalinity = 2300 μEq l^{-1}; pH = 7.98; pw Ca^{2+} concentration = 10.31 mmol/L; sedimentary $CaCO_3$ content = 80 wt.%; sedimentary $CaCO_3$ surface area = 10 m^2 g^{-1}; sediment porosity = 80%.

Pore water		Mineral surface	
Species	Concentration (μmol cm$_b^{-3}$)	Species	Concentration (μmol cm$_b^{-3}$)
$H_2CO_3^*$	0.0142	$>CO_3H^0$	0.0128
HCO_3^-	1.653	$>CO_3^-$	15.34
CO_3^{2-}	0.0937	$>CO_3Ca^+$	19.84
		$>CaOH_2^+$	35.15
		$>CaOH^0$	0.00212
		$>CaO^-$	2×10^{-18}
		$>CaHCO_3^0$	0.0377
		$>CaCO_3^-$	0.00903

core recovery due to decompression. Exchange reactions were invoked because simple solubility calculations accounting for decompression would imply a change in TA of only 112 μEq L^{-1} at these water depths, 20% of the observed change. If, however, the pH was held approximately constant during decompression due to exchange with mineral surfaces, a change in TA of 540 μEq L^{-1} is calculated, which is very near the observed value. No explanation for the large measured change in Ca^{2+} was provided. Nevertheless, these observations suggest that surface exchange reactions are capable of exchanging at least 440 to 1728 μEq L^{-1} (observed change minus the estimated decompression change of 112 μEq L^{-1} due to precipitation). As stated above, these surface exchanges were accompanied by a change in pH of 0.11.

Only a few fine-scale in situ surface pH measurements have been reported in the literature. At high $CaCO_3$, supersaturated sites, pH values decrease in the upper 0.5 to 1.0 cm by ~0.05 units on the Ceara Rise (Hales and Emerson, 1997a) and by 0.05 units at the equator in the central Atlantic (Archer et al., 1989). At supersaturated, low $CaCO_3$ sites in the western Atlantic, pH values decrease with sediment depth by ~0.3 units in the upper centimeter at the highest organic carbon rain rate site and by only 0.03 units at the lowest rain rate site (Hales et al., 1994). Thus, the change in pH observed in the surface 1 cm is similar in magnitude to the measured difference between the in situ and shipboard extractions.

The oxygen flux varies between the supersaturated, high $CaCO_3$ sites, from ~0.8 mol m^{-2} yr^{-1} on the Cape Verde Plateau to ~0.16 mol m^{-2} yr^{-1} at the Ceara Rise and Ontong Java Plateau. Assuming that this range of respiration produces a gradient in pH and carbonate system surface speciation as indicated above and that one proton is released for each metabolic CO_2 produced, the particle mixing rate that would neutralize the metabolic acidity generated is estimated to be 4.6 to 91 cm^2 yr^{-1}. Based on excess ^{234}Th measurements, numerous authors reported surface mixing rates ranging from several to as high as 33 cm^2 yr^{-1} (Cochran, 1985; DeMaster et al., 1985; Pope et al., 1996; Wheatcroft and Martin, 1996). While the upper value estimated here is larger than ^{234}Th observed values, the low value is within the range of reported values and supports the hypothesis that this mechanism may influence sedimentary dissolution rates.

5. CONCLUSIONS

The results presented here indicate that at undersaturated sea floor locations and at supersaturated locations that are characterized by low $CaCO_3$ (<5% by weight) contents, significant TA and Ca^{2+} fluxes are observed with in situ benthic flux chambers. These results are consistent with pore water results and previous diagenetic models. TA and Ca^{2+} benthic fluxes at sites that contain > 35 wt.% $CaCO_3$ and that are overlaid by supersaturated waters are greatly reduced from expected rates, however. We hypothesize that inorganic precipitation of $CaCO_3$ at the sediment surface and subsequent metabolic dissolution in the pore waters may explain these observations. Alternatively, surface exchange reactions with the $CaCO_3$ mineral may also impact the interpretation by buffering the concentration changes in the chambers or, when coupled with rapid particle mixing, pore waters. It is important to recognize that while the precipitation hypothesis is perhaps the most likely explanation for all of the observations, these possible explanations are not mutually exclusive. Under different circumstances each may contribute to varying degrees to the overall control of metabolic dissolution, $CaCO_3$ preservation and the net benthic fluxes of CA and Ca^{2+}.

Acknowledgments—We thank the captains and crews of the R/V L'Atalante and R/V Knorr for their assistance at sea on the 1991 Cape Verde expedition, the 1994 Ceara Rise expedition and the 1998 Cape Verde expedition. The authors thank David Archer, Marion Gehlen, Bill Martin and Alfonso Mucci for showing great interest in this work and for numerous comments about earlier versions of this manuscript. G. M. Nickles and C. Y. Robertson provided instrumentation support on the expeditions. Financial support was provided by the National Science Foundation grants OCE-9000323, OCE-9201896, OCE-9617297 and OCE-9911707.

Associate editor: A. Mucci

REFERENCES

Antia A. N., Koeve W., Fischer G., Blanz T., Schultz-Bull D., Scholten J., Neuer S., Kremling K., Kuss J., Hebbeln D., Bathmann U., Fehner U., and Zeitzschel B. (in press) Basin-wide particulate carbon flux in the Atlantic Ocean: Regional export patterns and potential for atmospheric CO_2 sequestration. *Global Biogeochem. Cycles*.

Archer D. (1991) Modeling the calcite lysocline. *J. Geophys. Res.* **96**, 17037–17050.

Archer D. and Maier-Reimer E. (1994) Effect of deep-sea sedimentary calcite preservation on atmospheric CO_2 concentration. *Nature* **367**, 260–263.

Archer D., Emerson S., and Reimers C. (1989) Dissolution of calcite in deep-sea sediments: pH and O_2 microelectrode results. *Geochim. Cosmochim. Acta* **53**, 2831–2845.

Berelson W. M., Hammond D. E., and Cutter G. A. (1990) In situ measurements of calcium carbonate dissolution rates in deep-sea sediments. *Geochim. Cosmochim. Acta* **54**, 3013–3020.

Broecker W. S. and Clark E. (2003) Pseudo dissolution of marine calcite. *Earth Planet. Sci. Lett.* **65**, 1–6.

Broecker W. S. and Takahashi T. (1966) Calcium carbonate precipitation on the Bahama Banks. *J. Geophys. Res.* **71**, 1575–1602.

Brzezinski M. A. (1985) The Si:C:N ratio of marine diatoms: Interspecific variability and the effect of some environmental variables. *J. Phycol.* **21**, 347–357.

Buchholtz–ten Brink M. R., Gust G., and Chavis D. (1989) Calibration and performance of a stirred benthic chamber. *Deep-Sea Res.* **36**, 1083–1101.

Cochran J. K. (1985) Particle mixing rates in sediments of the eastern equatorial Pacific: Evidence from ^{210}Pb, ^{239,240}Pu and ^{137}Cs distributions at MANOP sites. *Geochim. Cosmochim. Acta* **49**, 1195–1210.

Curry W. B. and Lohmann G. P. (1990) Reconstructing past particle fluxes in the tropical Atlantic Ocean. *Paleoceanography* **5**, 487–505.

DeMaster D. J., McKee B. A., Nittrouer C. A., Brewster D. C., and Biscaye P. E. (1985) Rates of sediment reworking at the HEBBLE site based on measurements of Th-234, Cs-137 and Pb-210. *Mar. Geol.* **66**, 133–148.

Emerson S. and Bender M. (1981) Carbon fluxes at the sediment-water interface of the deep-sea: Calcium carbonate preservation. *J. Mar. Res.* **39**, 139–162.

Emerson S., Grundmanis V., and Graham D. W. (1982) Carbonate chemistry in marine pore waters: MANOP sites C and S. *Earth Planet. Sci. Lett.* **61**, 139–162.

Gehlen M., Mucci A., and Boudreau B. (1999) Modelling the distribution of stable carbon isotopes in porewaters of deep-sea sediments. *Geochim. Cosmochim. Acta* **63**, 2763–2773.

Hales B. (1995) *Calcite Dissolution on the Sea Floor: An In Situ Study*. Ph.D. dissertation, University of Washington.

Hales B. and Emerson S. (1996) Calcite dissolution in sediments of the Ontong-Java Plateau: In situ measurements of porewater O_2 and pH. *Global Biogeochem. Cycles* **5**, 529–543.

Hales B. and Emerson S. (1997a) Calcite dissolution in sediments of the Ceara Rise: In situ measurements of porewater O_2, pH and $CO_{2(aq)}$. *Geochim. Cosmochim. Acta* **61**, 501–514.

Hales B. and Emerson S. (1997b) Evidence in support of first-order dissolution kinetics of calcite in seawater. *Earth Planet. Sci. Lett.* **148**, 317–327.

Hales B., Emerson S., and Archer D. (1994) Respiration and dissolution in the sediments of the western North Atlantic: Estimates from models of in situ microelectrode measurements of porewater oxygen and pH. *Deep-Sea Res.* **41**, 695–719.

Jahnke R. A. (1990) Early diagenesis and recycling of biogenic debris at the seafloor, Santa Monica Basin, California. *J. Mar. Res.* **48**, 413–436.

Jahnke R. A. (1998) Geochemical impacts of waste disposal on the abyssal seafloor. *J. Mar. Sys.* **14**, 355–375.

Jahnke R. A. and Christiansen M. B. (1989) A free-vehicle benthic chamber instrument for sea floor studies. *Deep-Sea Res.* **36**, 625–637.

Jahnke R. A. and Jahnke D. B. (2000) Rates of C, N, P and Si recycling and denitrification at the US Mid-Atlantic continental slope depocenter. *Deep-Sea Res.* **47**, 1405–1428.

Jahnke R., Heggie D., Emerson S., and Grundmanis V. (1982) Pore waters of the central Pacific Ocean: Nutrient results. *Earth Planet. Sci. Lett.* **61**, 233–256.

Jahnke R. A., Craven D. B., and Gaillard J.-F. (1994) The influence of organic matter diagenesis on $CaCO_3$ dissolution at the deep-sea floor. *Geochim. Cosmochim. Acta* **58**, 2799–2809.

Jahnke R. A., Craven D. B., McCorkle D. C., and Reimers C. E. (1997) $CaCO_3$ dissolution in California continental margin sediments: The influence of organic matter remineralization. *Geochim. Cosmochim. Acta* **61**, 3587–3604.

Martin W. R. and Sayles F. L. (1996) $CaCO_3$ dissolution in sediments of the Ceara Rise, western equatorial Atlantic. *Geochim. Cosmochim. Acta* **60**, 243–263.

Martin W. R., McNichol A. P., and McCorkle D. C. (2000) The radiocarbon age of calcite dissolving at the sea floor: Estimates from pore water data. *Geochim. Cosmochim. Acta* **64**, 1391–1404.

Milliman J. D., Troy P. J., Balch W. M., Adams A. K., Li Y.-H., and Mackenzie F. T. (1999) Biologically mediated dissolution of calcium carbonate above the chemical lysocline? *Deep-Sea Res.* **46**, 1653–1669.

Morris A. W. and Riley J. P. (1966) The bromide/chlorinity and sulphate/chlorinity ratio in sea water. *Deep-Sea Res.* **13**, 699–705.

Morse, J. W., D. K. Gledhill and Millero F. J. (in press) $CaCO_3$ precipitation kinetics in waters from the Great Bahama Bank: Implications for the relationship between Bank hydrochemistry and whitings. *Geochim. Cosmochim. Acta*.

Pope R. H., DeMaster D. J., Smith C. R., and Seltmann H. Jr. (1996) Rapid bioturbation in equatorial Pacific sediments: Evidence from excess ^{234}Th measurements. *Deep-Sea Res.* **43**, 1339–1364.

Rao A. and Jahnke R. A. (2002) Quantifying pore water exchange across the sediment-water interface in the deep sea with in situ tracer studies. AGU/ASLO Abstract, OS41A-04.

Redfield A. C., Ketchum B. H., and Richards F. A. (1963) The influence of organisms on the composition of seawater. In *The Sea, Vol. 2* (ed. M. N. Hill). Interscience, New York.

Reimers C. E., Jahnke R. A., and Thomsen L. (2001) In situ sampling in the benthic boundary layer. In *The Benthic Boundary Layer: Transport Processes and Biogeochemistry* (eds. B. P. Boudreau and B. B. Jørgensen), pp. 245–268. Oxford University Press, Oxford, UK.

Strickland J. D. H. and Parsons T. R. (1972) *A Practical Handbook of Seawater Analysis.* Bulletin 167. 2nd ed. Fisheries Research Board of Canada, Ottawa.

Tsunogai S., Nishimura M., and Nakaya S. (1968) Complexometric titration of calcium in the presence of larger amounts of magnesium. *Talanta* **15**, 385–390.

Ullman W. J. and Aller R. C. (1982) Diffusion coefficients in nearshore marine sediments. *Limnol. Oceanogr.* **27**, 552–556.

van Cappellen P., Charlet L., Stumm W., and Wersin P. (1993) A surface complexation model of the carbonate mineral-aqueous solution interface. *Geochim. Cosmochim. Acta* **57**, 3505–3518.

Wheatcroft R. A. and Martin W. R. (1996) Spatial variation in short-term (^{234}Th) sediment bioturbation intensity along an organic-carbon gradient. *J. Mar. Res.* **54**, 763–792.